iScience

CellPress
OPEN ACCESS

Article

Redox-responsive polyurethane-polyurea nanoparticles targeting to aortic endothelium and atherosclerosis

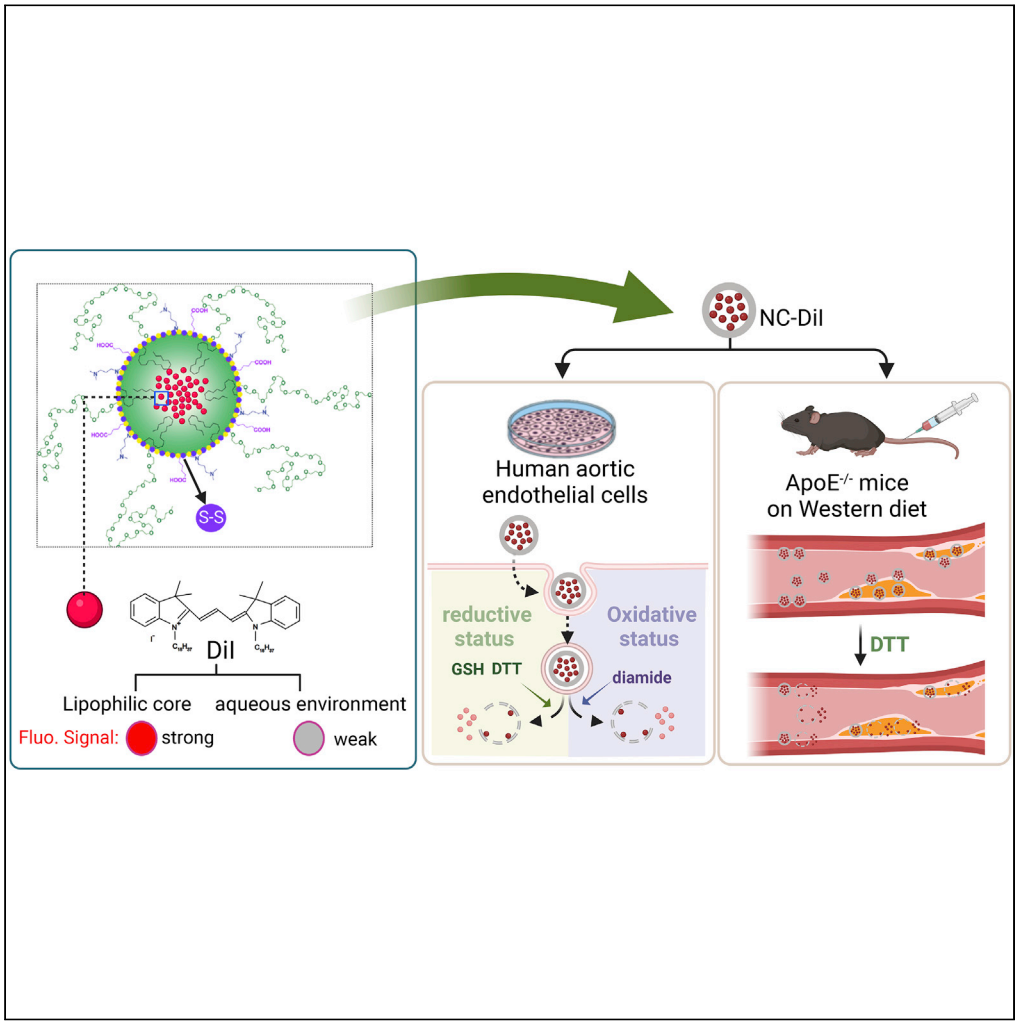

Yuxiang Zhou, David Hou, Cristina Cusco Marigo, ..., Josep Rocas, Naomi M. Hamberg, Jingyan Han

jingyanh@bu.edu

Highlights

Aortic endothelial dysfunction precipitates atherosclerosis and cardiovascular disease

Nano-capsules show high affinity to aortic endothelium and atherosclerotic lesions

Offering a nanomedical approach to deliver drugs to improve cardiovascular outcomes

Disulfide bonds enable control of drug release by changing thiol redox status

Zhou et al., iScience 25, 105390
November 18, 2022
https://doi.org/10.1016/j.isci.2022.105390

iScience

CellPress
OPEN ACCESS

Article

Redox-responsive polyurethane-polyurea nanoparticles targeting to aortic endothelium and atherosclerosis

Yuxiang Zhou,[1] David Hou,[1] Cristina Cusco Marigo,[2] Joaquín Bonelli,[2] Pau Rocas,[2] Fangzhou Cheng,[1] Xiaoqiu Yang,[1] Josep Rocas,[2] Naomi M. Hamberg,[1] and Jingyan Han[1,3,*]

SUMMARY

Aortic endothelial cell dysfunction is an early trigger of atherosclerosis, the major cause of the cardiovascular disease (CVD). Nanomedicines targeting vascular endothelium and lesions hold great promise as therapeutic solutions to vascular disorders. This study investigates the vascular delivery efficacy of polyurethane-polyurea nanocapsules (Puua-NCs) with pH-synchronized shell cationization and redox-triggered release. Fluorescent lipophilic dye DiI was encapsulated into Puua-NCs of variable sizes and concentrations. *In vitro* cellular uptake studies with human aortic endothelial cells showed that these Puua-NCs were taken up by cells in a dose-dependent manner. In apolipoprotein E-deficient mice fed a Western diet, a model of atherosclerosis, circulating Puua-NCs were stable and accumulated in aortic endothelium and lesions within 24 hours after intravenous administration. Treatment with thiol-reducing and oxidizing reagents disrupted the disulfide bonds on the surface of internalized NCs, triggering disassembly and intracellular cargo release. Ultimately, Puua-NCs are a potential redox-controllable cardiovascular drug delivery system.

INTRODUCTION

Despite tremendous advances in prevention, diagnosis, and intervention spurring improvements in patient outcomes, cardiovascular diseases (CVDs) such as heart attack, stroke, and aortic and coronary artery disease remain a leading cause of global death (Benjamin et al., 2017). There continues to be a pressing medical need for effective options to treat these devastating conditions. Nanoparticle (NP) delivery systems—engineered for the targeted delivery and controlled release of therapeutic agents—have emerged as promising tools to afford the targeted delivery of drugs to the cardiovascular system and to alleviate heart and vascular diseases; in addition, NPs can be employed for molecular imaging applications by targeting molecular markers of vascular diseases and facilitating targeted delivery of genomic editing technology[1,2] Specifically, NP delivery systems have the potential to[1]: improve the pharmacokinetic and pharmacodynamic properties of existing cardiovascular drugs[2]; deliver payloads (e.g., pharmacological agents, genetic materials, and stem cells) to specific disease sites of the heart and blood vessels; and[3] reduce the pathogenic factors of CVD (e.g., hyperlipidemia, oxidative stress, endothelial dysfunction, inflammation, and thrombosis).[3] Considering CVD is chronic, delivery systems providing the sustained and controlled release of cargoes to disease sites have broad prospects for condition management and have been intensively investigated.[4] In this regard, polymeric nanocapsules (NCs) have attracted considerable interest as drug carriers. NCs can now be made in various sizes (10-1000 nm in diameter) and shapes (sphere, disk, tube, and bowl); they consist of a hydrophobic core that retains drugs as well as a polymeric shell that facilitates the targeted delivery of drugs to their intended biological destinations by targeting moieties and controlling NC disassembly and drug release—such control is achieved by incorporating internal and external sensors to light, pH, and redox status.[5] Accordingly, the main advantages of NCs as drug carriers are encapsulated in their capacity for controlled, targeted drug delivery, stimuli-sensitive release, improved drug bioavailability, and mitigation of undesired side effects and toxicity.

In the present study, we focus on polyurea-polyurethane NCs (Puua-NCs), which have been well characterized as a multi-sensitive drug delivery system with pH-synchronized shell cationization and redox-triggered release.[6] Puua-NCs were originally devised for anticancer drug delivery[7,8] because of their utility in solid

[1]Vascular Biology Section, Evans Department of Medicine, Whitaker Cardiovascular Institute, Boston University School of Medicine, 650 Albany St. X 729, Boston, MA, USA

[2]Nanobiotechnological Polymers Division, Ecopol Tech S.L., L'Arboc, Spain

[3]Lead contact

*Correspondence: jingyanh@bu.edu

https://doi.org/10.1016/j.isci.2022.105390

tumor tissues, which contain an extracellular environment that is both acidic[9] and highly reductive, as reflected by thiol-disulfide balance.[10] To negotiate this environment, the outer shell of Puua-NCs is functionalized with both polycationic and anionic ionomers, conferring amphoteric properties that facilitate synchronized interaction in the pH range between physiological conditions and the tumor microenvironment. Notably, the surface charge of Puua-NCs remains neutral in circulation following intravenous administration, indicating that the Puua-NCs are able to avoid opsonization and sequestration by the mononuclear phagocytic system. This greatly prolongs the circulation half-life of the Puua-NCs, while, in the acidic tumor microenvironment, they become highly cationized and facilitate cellular uptake and endosomal release.[6] Furthermore, the presence of redox-sensitive disulfide bonds (-S-S-) on the Puua-NC surface promotes disassembly of internalized NCs in tumor cells because these disulfide bonds are reduced and disrupted in the highly reductive environment. Although Puua-NCs have a demonstrated capability for targeted delivery of hydrophobic and toxic anticancer drugs to various tumor cells and tissues, it remains unexplored whether Puma-NCs can be utilized as a redox-sensitive drug delivery device for the cardiovascular system.

The aortic endothelium, a monolayer of endothelial cells (ECs) lining the aortic lumen, acts not only as a gatekeeper to water and electrolytes via its selective permeability but also a critical player in maintaining vascular homeostasis; conversely, dysfunctional ECs cause vascular damage by disrupting barrier integrity; dampening vasoactive molecules, such as nitric oxide (NO); and igniting inflammation and oxidative stress, thereby driving the development of atherosclerosis, a major cause of CVD. Therefore, delivering therapeutic agents to aortic ECs holds great promise in reducing vascular endothelial damage, impeding atherosclerosis, and improving cardiovascular outcomes. However, several challenges hinder the widespread application of aortic ECs in basic and clinical cardiovascular research. First, similar to ECs in other vascular beds (e.g., arterioles, veins, capillaries), aortic ECs lack suitable cell surface receptors for viral vectors (e.g., adenoviral, lentiviral, and adeno-associated viral vectors) that are currently prime carriers of genetic materials, so almost all currently available viral vectors have no specific affinity to ECs.[11] Second, in contrast to ECs lining microvasculature or veins, aortic ECs are constantly exposed to pulsatile blood flow that generates drag forces and prevents interactions between NPs and ECs and subsequent cellular uptake. Third, even after being taken up by ECs, NPs are typically sequestered into endosomes and lysosomes for degradation, limiting the intracellular release of cargoes.

In this study, we demonstrate that Puua-NCs can be taken up by aortic ECs both *in vitro* and *in vivo*. In a mouse model of atherosclerosis, intravenously administered Puua-NCs concentrate in aortic atherosclerotic lesions; the disassembly of Puua-NCs delivered to aortic endothelium and atherosclerotic lesions is triggered by thiol reducing agents. These findings show that Puua-NC is a redox controllable drug delivery system for CVD.

RESULTS

Production and characterization of DiI-polyurethane-polyurea nanocapsules in various sizes

As a drug delivery system, the robustness of NCs in encasing therapeutic agents, targeting diseased sites, and controlling trafficking in cells is determined by their size, surface characteristics, and material composition. Because optimal NC size is critical to cellular uptake,[12] we generated Puua-NCs in three sizes, ranging from 10 to 300 nm in diameter. The synthesis and characterization of basic Puua-NCs have been reported in previous studies.[13,14] As illustrated in Figure 1A, synthesis consists of two steps: preparation of an amphiphilic cationic prepolymer, and nanoencapsulation of the drug of interest—in this case, the lipophilic fluorophore DiI. DiI-loaded Puua-NCs in three sizes were produced and characterized according to their size (Figure 1B), surface charge vs pH (Table 1), encapsulation efficiency, and loaded DiI (Table 2) using different characterization techniques (refer to supplemental information for details). Figure 1B shows that the particle size distributions exhibit monodispersity, with an average particle size of 14.15 $\pm$ 0.63, 170.20 $\pm$ 44.01, and 239.50 $\pm$ 99.78 nm, respectively, for small (NC-DiI-SS), medium (NC-DiI-MS), and large (NC-DiI-LS) sizes. We examined the NC concentration and DiI loading capacity for these three sizes and found a relatively high loading capacity for small NCs (0.86% vs 0.48% and 0.69% for medium- and large-sized NCs, respectively). An important feature of Puua-NCs is that their surfaces are amphiphilic and highly sensitive to small pH changes. At physiological pH~7.4 (e.g., in circulation), neutral hydrophilic corona formation enhances their stealth properties, while in acidic conditions (e.g., tumor microenvironment), the NC surface can be self-cationized, promoting uptake by tumor cells[13] Consistently, at pH = 7.4, the surface charge of the three NC groups as indicated by their ζ-potential values are 3.98 $\pm$ 0.48,

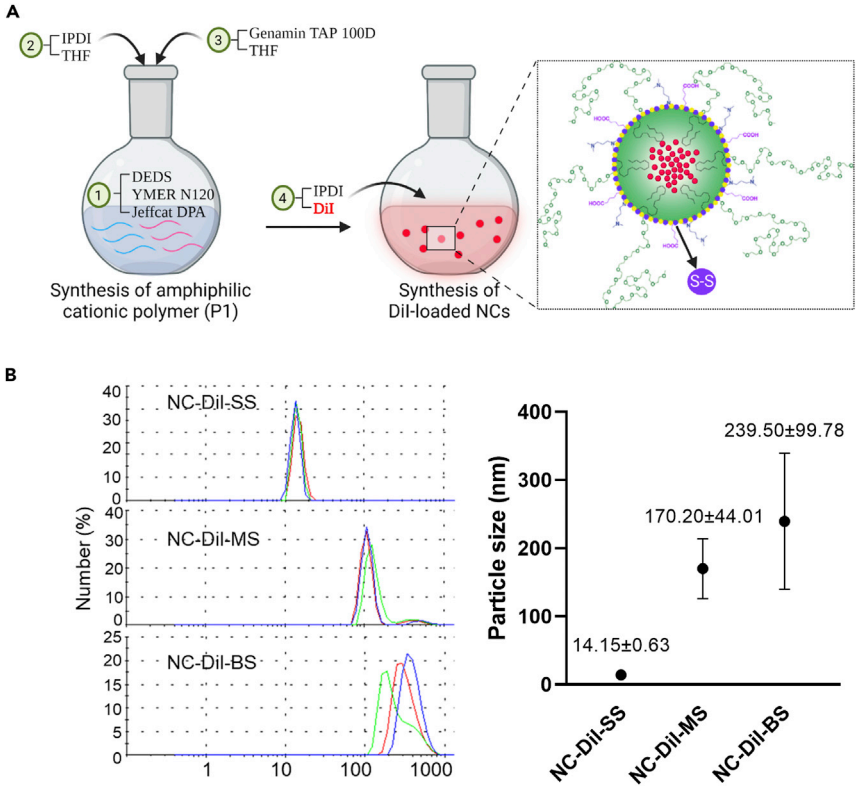

Figure 1. Synthesis of Puua-NCs and preparation in three sizes

(A) The synthetic process starts with the preparation of an amphiphilic cationic polymer (P1) by sequentially adding[1] DEDS, YMER N120, and Jeffcat DPA[2]; IPDI and THF); and[3] Genamin TAP 100D and THF. Thereafter, DiI in parallel with IPDI[4] is added to initiate nano-encapsulation. Red dots represent the synthesized NC-DiI. The magnified insert of the NC-DiI indicates its structure including the orientation of the hydrophobic and hydrophilic fractions of the prepolymer and the labile disulfide bonds on the shell, indicated by the purple dots.

(B) Particle size distribution of Puua-NCs of small (NC-DiI-SS), medium (NC-DiI-MS), and large (NC-DiI-BS) sizes, indicating monodispersity with an average particle size of 14.15 ± 0.63, 170.20 ± 44.01, and 239.50 ± 99.78 nm, respectively for small (NC-DiI-SS), medium (NC-DiI-MS), and large (NC-DiI-BS) sizes. Measured by dynamic light scattering (DLS).

9.96 ± 0.36, and −1.54 ± 0.32 mV for small, medium, and large capsules, respectively; while, at pH = 6.5, their values all significantly increase to 11.20 ± 0.31, 17.20 ± 0.53, and 17.60 ± 0.10 mV (Table 1), respectively. Given that, as is the case for solid tumors, atherosclerotic lesions typically display an acidic microenvironment due to chronic inflammation and hypoxia,[15] we speculate that this amphoteric property should promote cellular uptake in atherosclerotic lesions. To better control shell biodegradability and cargo release, the Puua-NC polymer wall was decorated with disulfide bonds that can be selectively cleaved by reductive molecules, such as reduced L-glutathione (L-GSH). This permits Puua-NCs to be highly stable in aqueous and protein-rich solutions but leaky in a reductive environment.[13] As a major strategy for redox-responsive drug delivery systems, disulfide bonds can be oxidized to a hydrophilic sulfoxide or sulphone by oxidating agents (e.g., HOCl, ONOOH), causing disulfide bond breakage and resultant NC shell disassembly.[16] Oxidative stress is a hallmark of cardiovascular disorders; in vascular cells within lesions, reactive

Table 1. ζ-potential of Puua-NCs in different sizes

Sample	ζ-Pot ± SD (mV) pH = 6.5	ζ-Pot ± SD (mV) pH = 7.4
NC-DiI-SS	11.20 ± 0.31	3.98 ± 0.48
NC-DiI-MS	17.20 ± 0.53	9.96 ± 0.36
NC-DiI-BS	17.60 ± 0.10	−1.54 ± 0.32

Table 2. DiI loading capacity (%)

Samples	[NCs] (mg/mL)	DiI Loading (mg/mL)	DiI Loading Capacity %
NCs-DiI-SS	55	0.4728	0.86
NCs-DiI-MS	40	0.2617	0.48
NCs-DiI-BS	55	0.38	0.69

oxygen species (ROS) are over-produced while GSH levels are reduced.[17] How cellular uptake and trafficking of Puua-NCs are affected by vascular redox status is currently unknown. Such knowledge could provide new insights into the application of redox-responsive drug delivery systems in cardiovascular medicine.

Polyurethane-polyurea nanocapsules can be taken up by aortic endothelial cells

We first characterized the endothelial uptake of Puua-NCs *in vitro*. It has been increasingly acknowledged that ECs from different vascular beds display distinct phenotypes in morphology, structure, and function, all of which are essential to the cellular uptake of nanoparticles.[18] To better recapitulate the binding and retention of Puua-NCs in aortic ECs, we chose to use human primary HAECs to perform the experiments described later in discussion. First, we examined how NC size affected endothelial uptake. As depicted in Figure 2A, a confluent HAEC monolayer was incubated with NC-DiI-SS (~20 nm, small-sized), NC-DiI-MS (~170 nm, medium-sized), and NC-DiI-BS (~245 nm, large-sized) at three different concentrations for 30 min, followed by the careful removal of unbound NCs and fixation. Endothelial uptake was then assessed by red fluorescence signals, indicative of DiI encapsulated in NCs. Figure 2B shows that, compared to the control polystyrene nanospheres (NPs), all three NC sizes showed significant uptake by HAECs at a concentration of 0.027 mg/mL, and the amount of NCs absorbed by HAECs increased with increasing NC concentration (0.270, 2.7 mg/mL). Quantification of the average number of NCs (Figure 2C) indicated that NC-DiI-MS (~175 nm) was the most robust in endothelial uptake. The small-sized NCs were less efficient in targeting ECs; but this endothelial uptake should be underestimated because, due to the small amount of DiI encapsulated individually in small-sized NCs (~20 nm), the fluorescence signal derived from encapsulated DiI might be too low to be detected during fluorescence imaging for a given set of exposure settings for all samples. Notably, the fluorescence signal reflected the total levels of NCs taken up by HAECs and could not, therefore, be used to differentiate between NCs bound to cell surfaces and NCs within cells.

Next, we evaluated NC retention in HAECs after incubation for different periods of time (0.5, 2, and 5 hrs). Figures 3A and 3B show middle- and large-sized Puua-NCs concentrated in HAECs and peaked at 2 hours, followed by a significant reduction. In contrast, the amount of small-sized Puua-NCs within HAECs continuously increased with time, although overall levels were not as high as the other two NCs. Taken together, these data (Figures 1, 2, and 3) suggest that Puua-NCs are rapidly taken up by HAECs regardless of particle size; the extent of cellular uptake and retention appear to be dependent on particle size, highlighting the accepted vital role of particle size in controlling cellular uptake and retention.[19] Following these results, we used medium-sized NCs that displayed more optimal endothelial uptake for the remaining *in vitro* experiments. Moving forward, it would be intriguing to further investigate this size-dependent effect of NCs on cellular uptake and intercellular trafficking in ECs. Such investigation should yield new insights into cardiovascular-targeted nano-drug delivery systems to achieve desired EC-NC interactions.

Polyurethane-polyurea nanocapsules can be taken up by aortic endothelium and atherosclerotic lesions in *ApoE*$^{-/-}$ mice

In vivo, vascular endothelium is constantly exposed to blood flow and changes in flow patterns, which are central contributory factors in vascular homeostasis and disease, such as with atherosclerosis.[20] Hemodynamic forces directly affect the interaction between ECs and circulating nanoparticles.[21] To assess the targeting efficiency of Puua-NCs to aortic ECs and atherosclerosis *in vivo*, *ApoE*$^{-/-}$ mice were fed a WD for two months to develop aortic lesions. The mice were then intravenously administered with control NPs (200 nm in diameter), NC-DiI-SS (~20 nm in diameter), and NC-DiI-BS (~240 nm in diameter) at a dose of 100 mg of polymer/kg of bodyweight for 24 hr. The mice were then subjected to *en face* aortic confocal microscopy to image their aortic endothelium and lesions (Figure 4A). The representative images shown in Figure 4B demonstrate vigorous endothelial targeting for both small- and large-sized NCs compared to that barely detectable for

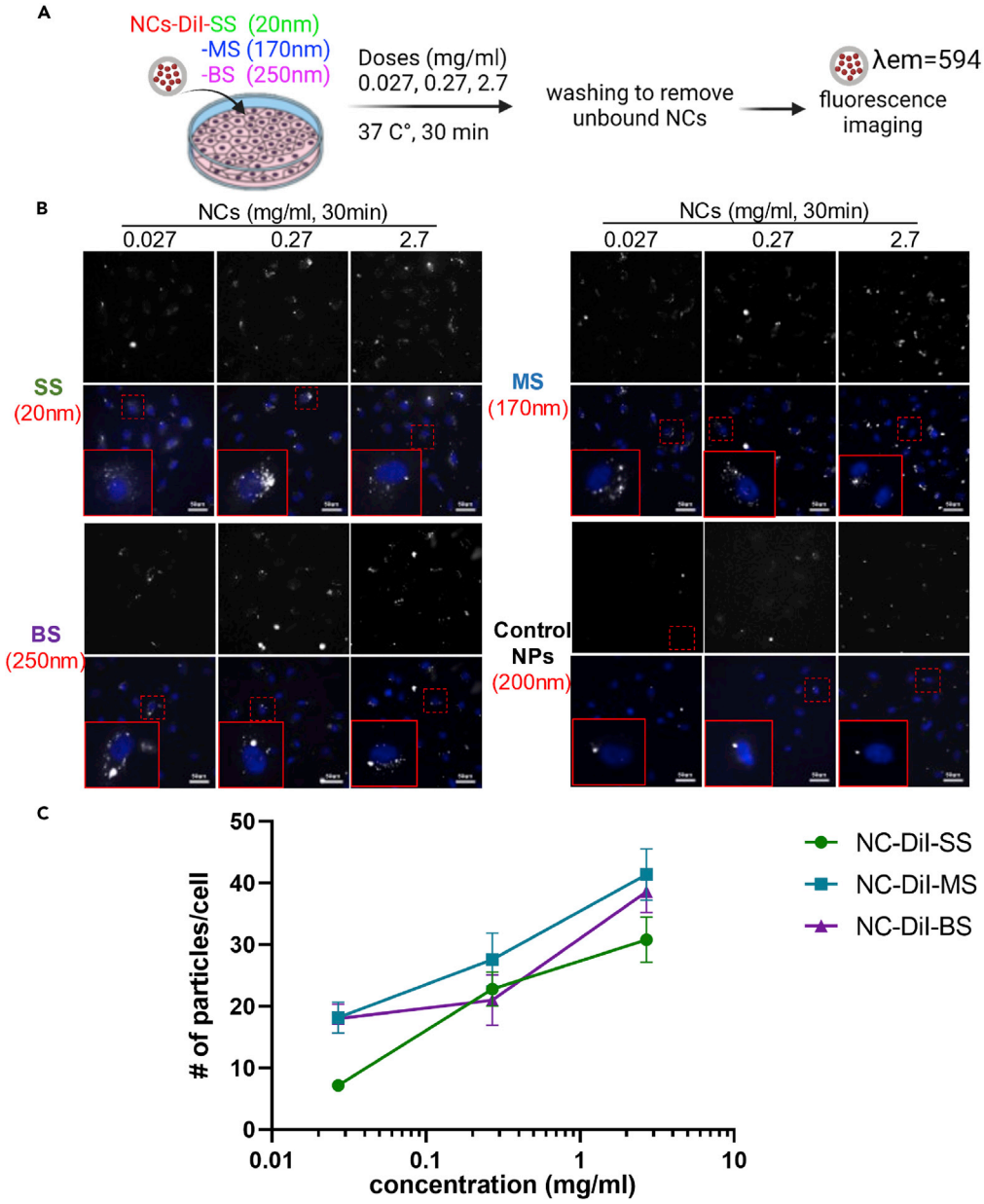

Figure 2. *In vitro* endothelial uptake of Puua-NCs of variable sizes and concentrations

(A) Confluent HAECs were incubated with control polystyrene nanoparticles (control NPs, 200 nm), and NCs-DiI in varying sizes (20, 175, 250 nm) and concentrations (0.027, 0.27, 2.7 mg/mL) as indicated at 37C° for 30 min. Cells were then placed on ice, carefully washed, fixed, and subjected to fluorescence microscopy.

(B) Grayscale fluorescence images show the representative control NPs or NCs-DiI taken up by HAECs, which are counterstained with DAPI (blue color) to indicate the nuclei. The insets are the magnified view of the area outlined by the red dashed lines.

(C) Quantification of Puua-NCs taken up by HAECs within 30 min as a function of NP concentrations. Data are expressed as mean # of NCs per cell ± SE from 5 to 7 randomly taken images, and representative of three independent experiments. Scale bar: 50 μm.

the control NPs. Compared with the bright and punctuate fluorescence signals of large-sized NCs, the signals of small NCs (20 nm in diameter) were weak and diffused, very likely owing to their diminutive size. Strikingly, NC-DiI-BS was highly accumulated in the aortic lesions (Figure 4C). These data strongly indicate the vigorous vascular endothelial targeting efficiency of Puua-NCs *in vivo*, potentially making them a candidate for drug

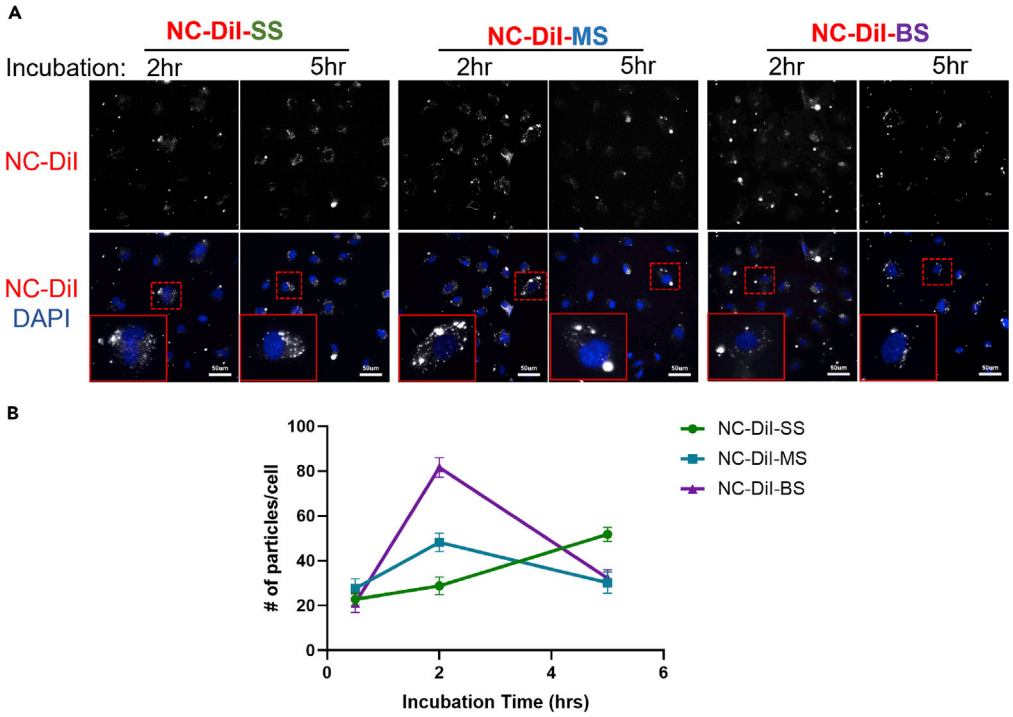

Figure 3. Effect of time of incubation on endothelial uptake of Puua-NCs in three sizes

(A) Confluent HAECs are incubated with NCs-DiI of three sizes as indicated at 37°C for 0.5, 2, and 5 hrs. The concentration of NCs-DiI was 0.27 mg/mL for all tested groups. Grayscale images show the representative NCs taken up by HAECs, which were counterstained with DAPI to indicate the nuclei.

(B) Quantification of NCs-DiI uptake within different periods of incubation time as indicated. Data are expressed as mean # of NCs per cell ± SE from 5 to 7 randomly taken images, which are representative of three independent experiments. Scale bar: 50 μm.

delivery in a cardiovascular system. The vascular targeting of nanoparticles has been a major hurdle limiting practical applications. Current cardiovascular targeting strategies involve functionalizing the NP surface with targeting ligands, such as antibodies or fragments against endothelial surface molecules (e.g., PECAM1),[21] to enhance NP binding affinity with endothelium. Despite lacking endothelial targeting moieties, Puua-NCs display excellent *in vivo* targeting efficiency for aortic ECs and lesions. This might be attributed to their unique surface properties, including:[1] a dangled hydrophilic polyurethane network, which protects NCs from quick phagocytic elimination and prolongs circulatory retention; and[2] pH-synchronized shell cationization, which enhances the affinity between positively charged NCs and negatively charged cell plasma membranes, facilitating cellular uptake and internalization[6] In addition to their efficient uptake by aortic endothelium and lesions, Puua-NCs also accumulated in other tissues, including lung tissue and liver tissue (Figure S9). We observed that Puua-NCs had a greater affinity for lung tissue than control NPs; conversely, Puua-NCs were taken up by hepatic tissues to a much less extent than control NPs. The function of liver is to remove foreign substances from the body, including NPs from the bloodstream. This efficient but non-specific accumulation of NPs in hepatic tissues poses a significant challenge for those drug delivery systems that target non-liver tissues, such as the cardiovascular system.[22] The structural and biochemical properties of Puua-NCs may prevent them from being trapped in the liver, prolonging their circulating half-life and allowing them to effectively target aortic vessels and lesions. Future studies are needed to investigate whether functionalizing Puua-NCs with vascular target ligands further improves Puua-NC vascular targeting efficacy. Considering that the aortic endothelium is a single-cell lining, and that conventional fluorescence microscopy of aortic cross-sections cannot fully image Puua-NCs concentrated in the endothelium, we performed confocal imaging of whole mount *en face* aorta preparations. This allowed the visualization of wide areas of the luminal vessel surface and rigorous analysis of NC uptake by the endothelium and lesions. ECs could be identified by their nuclei, which are large, spherical, and contain heterochromatin granules. Encapsulated cargo release of Puua-NCs in human aortic endothelial cells is controlled by manipulating thiol redox status.

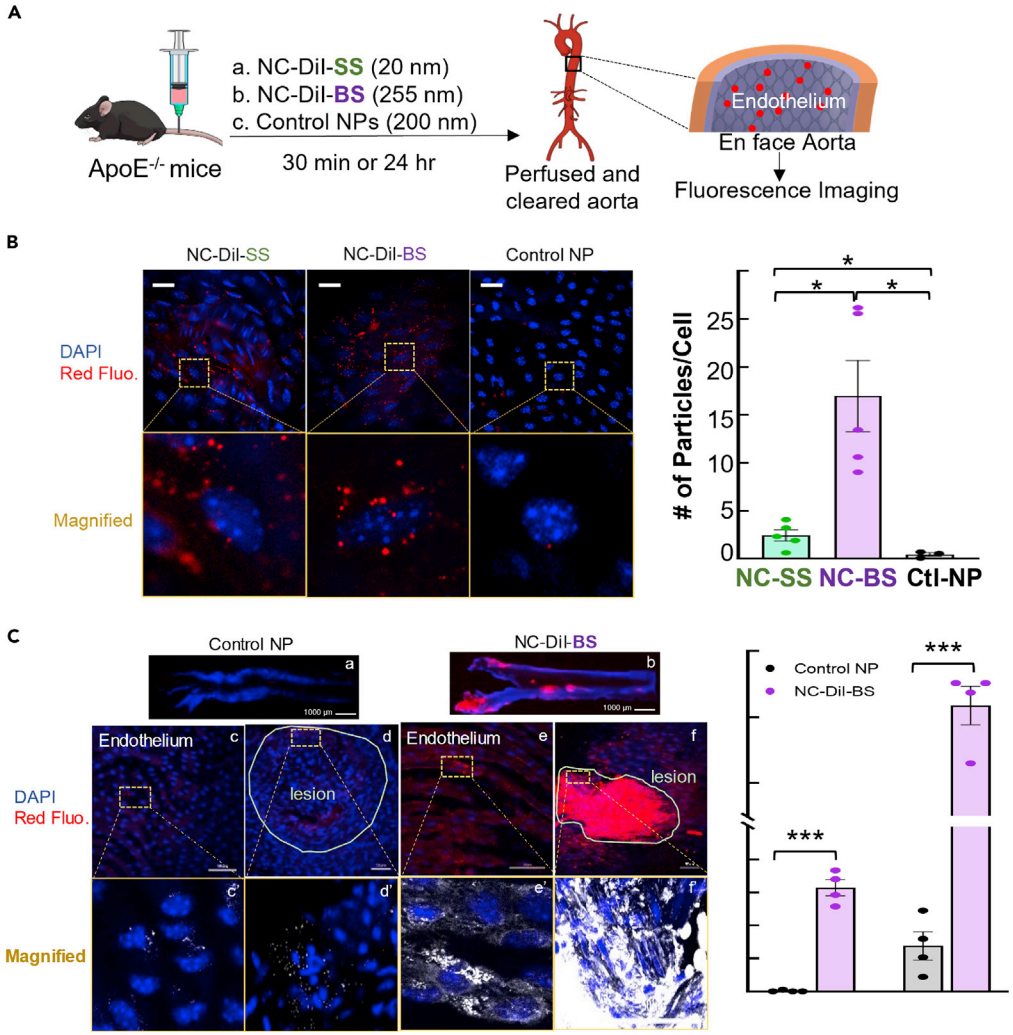

Figure 4. NC-Dil can be taken up by aortic endothelial cells and atherosclerotic lesions in ApoE$^{-/-}$ mice after intravenous administration

(A) The schematic describes the experimental process to assess *in vivo* vascular uptake of Puua-NCs in ApoE$^{-/-}$ mice after intravenous injection. NCs-Dil and control fluoresbrite® NPs (100 mg /kg body weight) were intravenously injected for 30 min (B) or 24 hours (C), followed by transcardial perfusion to remove blood and unbound NCs or NPs; thereafter the prepared *en face* aorta were subjected to fluorescence microscopy.

(B) Representative *en face* fluorescence images show aortic endothelial uptake of NC-Dil-SS, NC-Dil-BS, and control NPs in 30 min in ApoE$^{-/-}$ mice on the normal chow diet. The insets magnify the areas outlined in dashed lines. DAPI-counterstained nuclei showed several heterochromatin particles under the nuclear envelope, a nuclear feature of endothelial cells. Bar scale: 50 μm.

(C) Representative *en face* fluorescence images showing uptake of NCs-Dil by aortic endothelium and lesions in Western diet-fed ApoE$^{-/-}$ mice during 24 hrs after *i.v.* injection. Red fluorescent signals from NC-Dil-BS were highly accumulated in aortic endothelium (b, e) and aortic lesions (b, f), whereas minimal signals derived from control NPs were detected (a, c, and d). *$p < 0.05$, ***$p < 0.001$, N = 4.

Puua-NCs were designed to achieve redox-responsible disassembly and cargo release by incorporating liable disulfide bonds in the cross-linked prepolymers on the shell surface. Using *in vitro* fluorescence resonance energy transfer, Cusco et al. demonstrated that the addition of reducing agent glutathione (GSH) to a solution containing Puua-NCs triggered the NC breakdown and release of encapsulated cargoes[6] To test whether internalized NCs can be disassembled in HAECs with intracellular GSH levels of approximately 1-2 mM,[23] we exploited a unique feature of the organic fluorophore DiI, a lipophilic fluorescent cargo whose fluorescence signal (λ_{ex^*} = 549 nm, λ_{em^*} = 565 nm) is strong and punctuates when incorporated

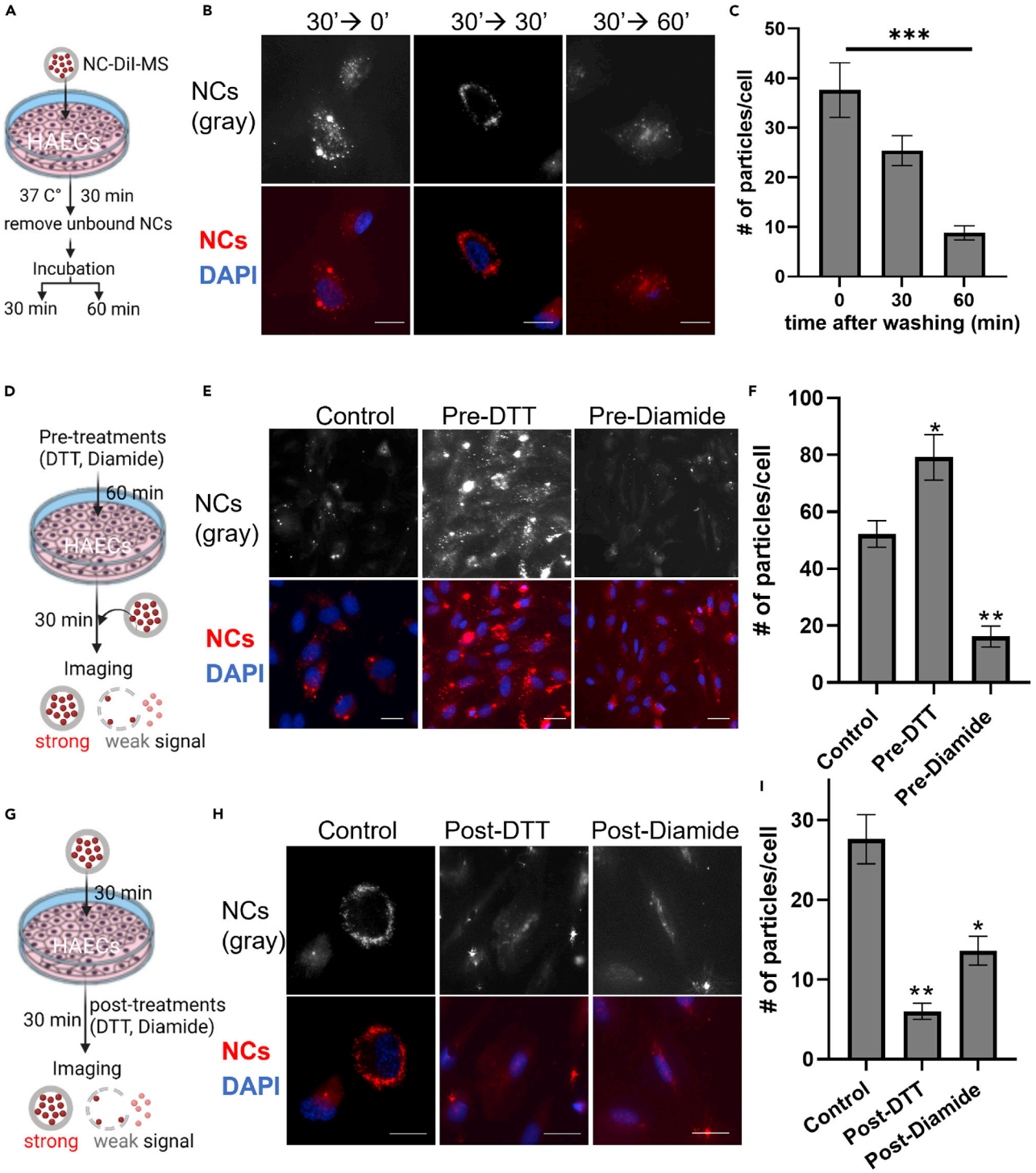

Figure 5. Puua-NCs disassembly can be controlled by redox status in endothelial cells

(A–C) DiI encapsulated in Puua-NCs were diffused in HAECs with increasing incubation time. NCs-DiI-MS (0.27 mg/mL) were incubated with confluent HAECs for 30 min, carefully washed to remove unbound NCs, and incubated with fresh medium for 30 or 60 min. The fluorescent signal of DiI encapsulated in NCs was imaged, and the number of NCs containing punctual and bright DiI dye signals were quantified and expressed as mean ± SE/cell of 5 randomly taken images (n = 5).

Figure 5. *Continued*

(D–I) The thiol reducing and oxidizing agents—dithiothreitol (DTT) and diamide, respectively—can stimulate Puua-NC disassembly in ECs. Pre- (D–F) or post- (G–I) treatments of DTT (1 mM) and diamide (50 μM) were used to disrupt disulfide bonds on the NC shell. The fluorescent signal of DiI dye encapsulated in NCs was imaged and the number of intact NCs was quantified and expressed as mean ± SE/cell of 5 randomly taken images (n = 5). Scale bar is 20 nm. *p < 0.05, **p < 0.01 compared with control group, unless otherwise indicated.

in the hydrophobic core of an NC, but is quenched by water molecules when DiI is released into cytosol, resulting in the fluorophore becoming weak and diffused.[24] Figure 5A shows HAECs that were pulse treated for 30 mins with NC-DiI-MS (0.27 mg/mL). The red fluorescence signal of cargo DiI was imaged 30 and 60 min after pulse treatment. We found that the fluorescence signal of NC was bright and punctuated immediately after incubation but became diffused and evenly distributed in cytosol over 60 min (Figure 5B). The number of internalized NCs with bright fluorescent signal was significantly reduced (Figures 5C, 37.6 ± 5.5, 25.4 ± 3.0, and 8.8 ± 1.4/cell for 0, 30, and 60 min, post-treatment, respectively, p = 0.0002). These data clearly indicate that DiI originally retained in the core compartment of NCs is released, supporting the notion that internalized NCs are disassembled within ECs, but the loss of the DiI fluorescence signal may be due to other causes, such as the "proton sponge effect," in which cationized NCs in acidic endosomes destabilize the membrane, leading to the disruption of endosomes and thus release of DiI. NCs may also undergo degradation in the lysosome or efflux from the cell. To further test whether the disassembly of Puua-NCs is controlled by the thiol redox status within ECs, we pre-treated HAECs with the thiol reducing agent DTT (1 mM) and the oxidizing agent diamide (50 μM) for 60 min, and then washed the cells with fresh medium to remove the reducing and oxidizing agents. Thereafter, cells were incubated with DiI-NC-MS (0.27 mg/mL) for 30 min, followed by washing to remove unbound NCs, fixation, and fluorescence microscopy (Figure 5D). Under a DTT-induced thiol reductive environment, internalized Puua-NCs were efficiently disassembled and released cargo DiI, as reflected by the diffused fluorescence signal. Interestingly, cellular uptake of NCs was markedly enhanced, as demonstrated by the significant increase in particle number per cell compared with the control group (Figures 5E and 5F, 52.2 ± 4.68 vs 79.2 ± 7.965, p = 0.037). In a diamide-induced thiol oxidative intracellular environment, however, Puua-NCs underwent massive degradation without stimulated cellular uptake, as evidenced by the dramatic decrease in the number of NCs remaining in cells (52.2 ± 4.68 vs 16.2 ± 3.69, p = 0.008). This clearly shows that intracellular redox status is critical to the cellular uptake of redox-responsive NCs. More importantly, both thiol reductive and oxidative intracellular environments, especially the latter, are hallmarks of diseased vascular cells and atherosclerotic lesions,[25] and may facilitate the drug release from Puua-NCs. This opens up particularly promising avenues for improving the efficiency of drug delivery to diseased vascular cells with minimal impact on healthy cells.

We tested the possibility of controlling the disassembly of internalized Puua-NCs using thiol reducing and oxidizing reagents. HAECs were incubated with NC-DiI-MS (0.27 mg/mL) for 30 min, washed to remove unbound NCs, and treated with DTT (1 mM) or diamide (50 μM) for 30 min before undergoing fluorescence microscopy (Figure 5G). Excitingly, we found that both DTT and diamide were able to trigger NC disassembly and consequent cargo release, as reflected by the significant reduction in particle numbers remaining in cells and the weak and diffused red fluorescence signal of cargo DiI (Figures 5H and 5I, 27.6 ± 3.08, 6.00 ± 1.00, and 13.6 ± 1.81 for the control group, post-DTT group, and post-diamide group, respectively).

Taken together, these results support the hypothesis that disulfide bonds can be disrupted by both reducing and oxidizing agents, allowing for more effective delivery of drugs by manipulating intracellular redox status. This is especially important for delivering drugs to diseased vascular endothelium and lesions, where GSH levels are suppressed but oxidative stress persists.[25]

Drug release of polyurethane-polyurea nanocapsules in aortic endothelium and lesions can be controlled by thiol reducing agent

Extending our *in vitro* EC study (Figure 5), we investigated whether *in vivo* administration of reducing agents could facilitate the disassembly of Puua-NCs accumulated in aortic endothelium and lesions. This test was critical for determining whether Puua-NCs could be utilized in cardiovascular medicine. As depicted in Figure 6A, *ApoE*$^{-/-}$ mice fed a two-month WD were intravenously administered NC-DiI-BS (100 mg of polymer components/kg of bodyweight). After 24 hrs, they were administered DTT or saline (as a control) for 30 min prior to aortic *en face* fluorescence microscopy. In the DTT-treated group, the fluorescence signal of cargo DiI was weakened in endothelium and massively diminished in lesions. This

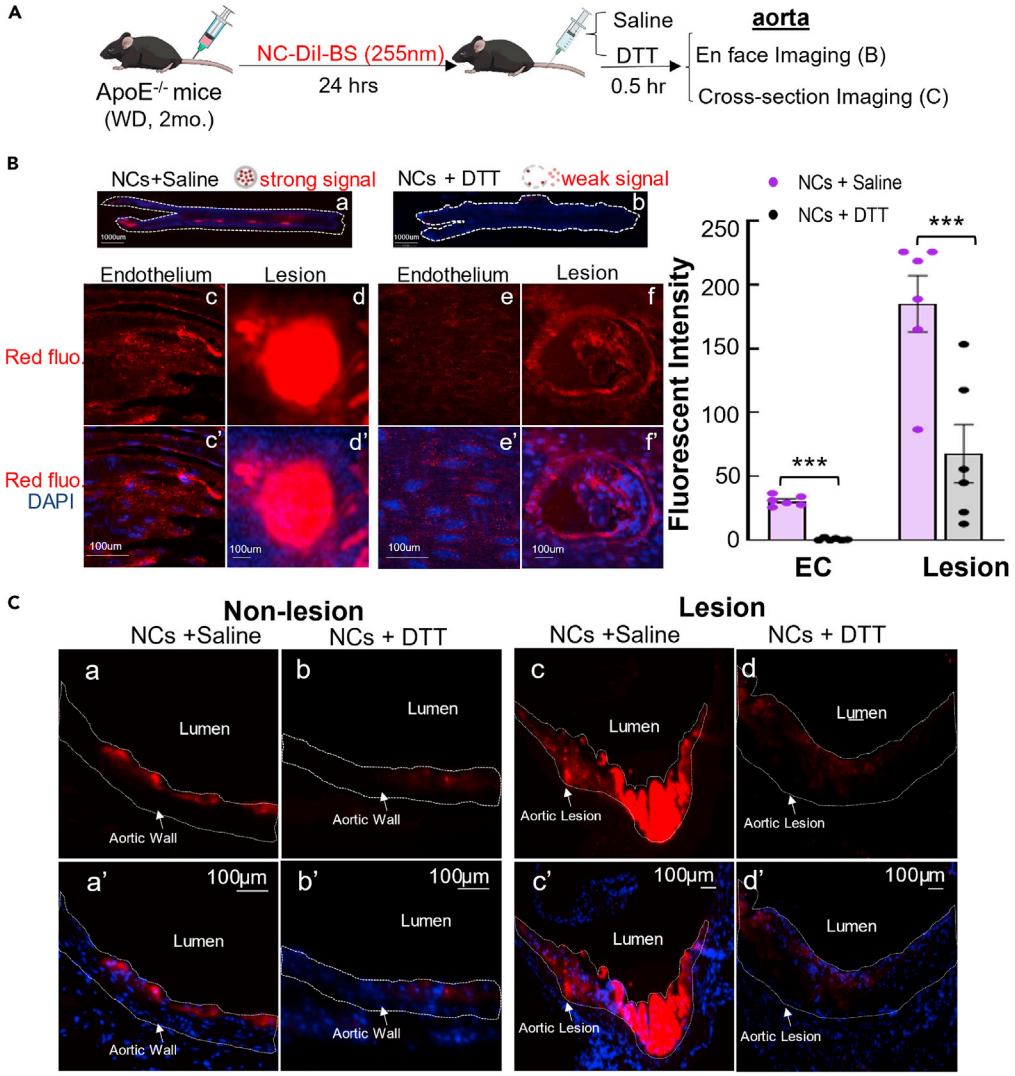

Figure 6. Thiol reducing agent can trigger the disassembly of NCs-Dil taken up by aortic endothelial cells and atherosclerotic lesions in ApoE$^{-/-}$ mice

(A) The schematic describes the experimental process to evaluate the effect of DTT (0.77 mg/Kg, i.v., 30 min) on the disassembly of NC-Dil-BS (100 mg of NCs/Kg, i,.v., 24 hrs) in aortic vessels of ApoE$^{-/-}$ mice fed Western diet for 2 months.

(B) *En face* fluorescent images of the aorta and quantifications of the fluorescent (fluo.) signals of DiI in the saline group (a, c, d, c', d') and the DTT-treated group (b, e, f, e', f'). N = 6, scale bar: 1000 um in (a) and (b); 100 um in (c, d, e, f). ***p < 0.001.

(C) representative images of the cross-section of aorta showing the NCs accumulated aortic wall without (a, a', b, b') or with lesions (c, c', d, d').

suggested that *in vivo* Puua-NC-mediated drug delivery to aortic endothelium and lesions could be effectively controlled by thiol reducing reagents. It is worth noting that, 24 hrs after NC-Dil-MS administration, a significant amount of NCs accumulated in the aortic endothelium, and lesions remained responsive to DTT treatment. This highlighted the excellent stability of NCs in circulation, as well as their prolonged retention in ECs and lesions; both of these qualities are essential for the development of effective redox-responsive drug-delivery nanodevices for the cardiovascular system.

DISCUSSION

We present both *in vitro* and *in vivo* evidence showing that Puua-NCs form a redox-controllable nano-drug delivery system that targets vascular endothelium and atherosclerotic lesions, as sumarized in Figure 7. This

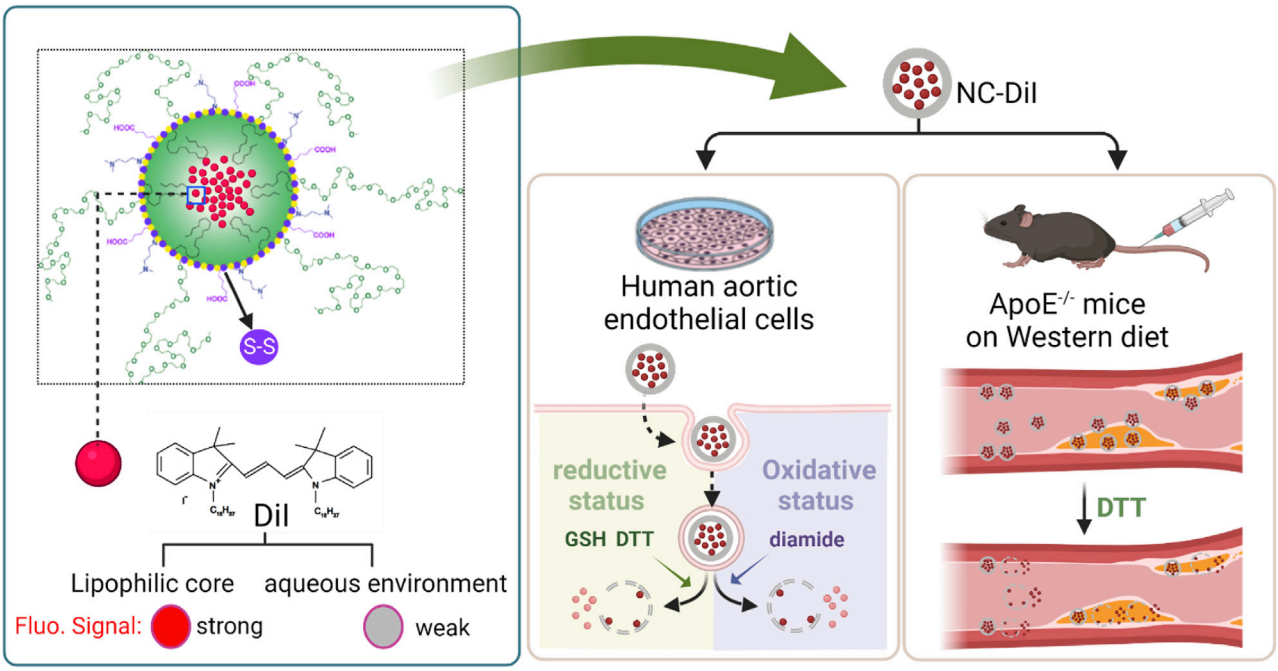

Figure 7. Puua-NCs effectively target aortic endothelial and atherosclerotic lesions and control their disassembly by manipulating intracellular thiol redox status

Prepared NC-DiI is given to HAECs and ApoE$^{-/-}$ mice intravenously. Note the DiI cargo in the NC-DiI, as indicated by the red dots in the center. DiI retained in the lipophilic core of NCs show a strong fluorescent (fluo.) signal, while DiI released into aqueous environment exhibits a weak signal. Thiol redox status in endothelial cells is altered via GSH, DTT, and diamide treatments. After 24 hours of NC-DII treatment, DTT was administered intravenously to the mice.

system should prove a powerful tool in the delivery of pharmaceuticals and genetic materials to damaged cardiovascular tissue in a controlled manner. The versatile and scalable Puua-NCs were initially designed for the effective delivery of anticancer drugs to tumor tissues (Cusco et al., 2016). Owing to their unique features, including pH-synchronized shell cationization and redox-sensitive release, Puua-NCs have been proven to form a potent drug-delivery nanodevice capable of guiding specific anti-cancer molecules to an acidic tumor microenvironment and potentiating drug effects while reducing systemic toxicity[14,26,27] To the best of our knowledge, this study is the first to evaluate the capability of Puua-NCs to target aortic endothelium and lesions in an animal model of atherosclerosis. As summarized in Figure 1, the synthetic method used in this study generates a wide range of prepolymers with preferred physicochemical properties by simply modifying the type, ratio, and concentration of starting monomers. In this case, a specifically designed prepolymer decorated with amphiphilic groups and disulfide bonds undergoes self-emulsification to encapsulate drugs and finely tune the NC size from 15 to 300 nm. NCs in three sizes (average diameters of 20, 175, and 255 nm) are all vigorously taken up by ECs to slightly different degrees, depending on both dose and incubation time (Figures 1, 2, and 3). Many variables, including NC size, shape, charge, biodegradable bonds, and targeting ligands, impact NC uptake into ECs.[28,29] Based on the *in vitro* and *in vivo* findings (Figures 2, 3, 4, 5, and 6), we hypothesize that the presence of the polyethylene glycol (PEG) chains and the neutral to weak cationic charges on the surface of NCs may reduce opsonization and phagocytosis, thereby prolonging their half-life in the circulation. The present study is focused on evaluating the ability of Puua-NCs to target vascular cells and lesions and to release the encapsulated drugs in a redox controllable manner, which provides strong evidence supporting their potential applications in cardiovascular medicine. However, it is still unclear how Puua-NCs have a high efficacy in targeting vascular endothelium and atherosclerotic lesions. We speculate that vascular oxidative stress and inflammation occur in aortic endothelium and lesions under atherogenic conditions, resulting in an acidic microenvironment that may promote the protonation of the NC surface and enhance their cellular uptake; the hydrophobic nature of NCs could also play a role in the accumulation of atherosclerotic lesions. When Puua-NCs are internalized into endosomes, they can be further protonated under the acidic endosomal environment; the resultant strong cationic charges on the shell thus facilitate the NCs to escape from endosome; in the cytosol, both thiol reducing and oxidizing agents (e.g., GSH, DTT, ROS) can disrupt the disulfide bonds

that link NC polymers, leading to NC breakdown and payload release (Maillard et al., 2021; Pérez-Hernández et al., 2021; Bonelli et al., 2022). In summary, the presented redox-responsive Puua-NCs demonstrate robustness in targeting vascular endothelium and atherosclerotic lesions, as well as in the redox-controlled release of the encapsulated payload. This versatile, scalable, and targeting ligand-free nanocapsule system should become an effective drug delivery device, targeting the cardiovascular system to combat vascular diseases.

Limitations of the study

This study assesses the aortic endothelial uptake efficacy of Puua-NCs, which is a well-characterized drug delivery nanodevice with robust tumor targeting efficiency[7,8,24] Therefore, the underlying molecular basis of the NC-EC interaction and intracellular trafficking is not explored; this warrants further investigation. Second, Puua-NCs demonstrate a high targeting efficiency against vascular ECs and lesions, even though they are not decorated with EC-targeting ligands (e.g., CD31 antibody) on their surface—the primary strategy used in devising endothelium-targeted nanocarriers. It remains unclear whether this high targeting efficiency is specific to ECs and lesions, and if so, how Puua-NCs recognize and interact with ECs and atherosclerotic lesions *in vivo*.

STAR★METHODS

Detailed methods are provided in the online version of this paper and include the following:

- KEY RESOURCES TABLE
- RESOURCE AVAILABILITY
  - Lead contact
  - Materials availability
  - Data and code availability
- EXPERIMENTAL MODEL AND SUBJECT DETAILS
  - Mouse model of atherosclerosis
  - Cell culture
- METHOD DETAILS
  - Synthesis of amphiphilic cationic polymer (P1)
  - Synthesis of Puua-NC-DiI
  - Treatments
  - Whole mount *en face* aorta preparation
  - Microscopy and quantification of NCs taken up by HAECs and aorta in *ApoE*$^{-/-}$ mice
- QUANTIFICATION AND STATISTICAL ANALYSIS

SUPPLEMENTAL INFORMATION

Supplemental information can be found online at https://doi.org/10.1016/j.isci.2022.105390.

ACKNOWLEDGMENTS

The authors wish to acknowledge the Boston University Cellular Imaging Core for the use of its instruments and technical assistance. All graphics are created with BioRender.com. Funding: This work was supported by the National Institutes of Health (R01HL137771 to J.H., R21AG058983 to J.H., R21AA026922 to J.H, and 1UL1TR001430 to BU CTSI); the Evans Medical Foundation (to J.H.); and the Boston University Undergraduate Research Opportunity Program (to Y.Z., F.Z., X.Y.).

AUTHOR CONTRIBUTIONS

YZ, DH, CCM, JB, FC, XY, and JH carried out the experiments. YZ, DH, FC, XY, and YZ analyzed the data. YZ, DH, and JH wrote the article. JR and JH conceived the original idea and supervised the project. JH obtained the funding. All authors contributed to the article and approved the submitted version.

DECLARATION OF INTERESTS

The authors declare no competing interests.

Received: March 14, 2022
Revised: July 23, 2022
Accepted: October 14, 2022
Published: November 18, 2022

REFERENCES

1. Zhang, X., Jin, H., Huang, X., Chaurasiya, B., Dong, D., Shanley, T.P., and Zhao, Y.Y. (2022). Robust genome editing in adult vascular endothelium by nanoparticle delivery of CRISPR-Cas9 plasmid DNA. Cell Rep. *38*, 110196.

2. Atukorale, P.U., Covarrubias, G., Bauer, L., and Karathanasis, E. (2017). Vascular targeting of nanoparticles for molecular imaging of diseased endothelium. Adv. Drug Deliv. Rev. *113*, 141–156.

3. Han, J., Goodman, J., Zhang, M., and Li, Z. (2022). Chapter 8: Cardiovascular Drug Delivery in Organelle and Molecular Targeting (CRC press, Taylor & Francis Group), pp. 279–307.

4. Park, K. (2014). Controlled drug delivery systems: past forward and future back. J. Control. Release *190*, 3–8.

5. Lee, J.H., and Yeo, Y. (2015). Controlled drug release from pharmaceutical nanocarriers. Chem. Eng. Sci. *125*, 75–84.

6. Cuscó, C., Garcia, J., Nicolás, E., Rocas, P., and Rocas, J. (2016). Multisensitive drug-loaded polyurethane/polyurea nanocapsules with pH-synchronized shell cationization and redox-triggered release. Polym. Chem. *7*, 6457–6466.

7. Pérez-Hernández, M., Cuscó, C., Benítez-García, C., Bonelli, J., Nuevo-Fonoll, M., Soriano, A., Martínez-García, D., Arias-Betancur, A., García-Valverde, M., Segura, M.F., et al. (2021). Multi-smart and scalable bioligands-free nanomedical platform for intratumorally targeted tambjamine delivery, a difficult to administrate highly cytotoxic drug. Biomedicines *9*, 508.

8. Bonelli, J., Ortega-Forte, E., Vigueras, G., Bosch, M., Cutillas, N., Rocas, J., Ruiz, J., and Marchán, V. (2022). Polyurethane–polyurea hybrid nanocapsules as efficient delivery systems of anticancer Ir (iii) metallodrugs. Inorg. Chem. Front. *9*, 2123–2138.

9. Gerweck, L.E., Vijayappa, S., and Kozin, S. (2006). Tumor pH controls the in vivo efficacy of weak acid and base chemotherapeutics. Molecular cancer therapeutics *5*, 1275–1279.

10. Kuppusamy, P., Li, H., Ilangovan, G., Cardounel, A.J., Zweier, J.L., Yamada, K., Krishna, M.C., and Mitchell, J.B. (2002). Noninvasive imaging of tumor redox status and its modification by tissue glutathione levels. Cancer Res. *62*, 307–312.

11. Shimamura, M., Nakagami, H., Sanada, F., and Morishita, R. (2020). Progress of gene therapy in cardiovascular disease. Hypertension *76*, 1038–1044.

12. Chithrani, B.D., and Chan, W.C.W. (2007). Elucidating the mechanism of cellular uptake and removal of protein-coated gold nanoparticles of different sizes and shapes. Nano Lett. *7*, 1542–1550.

13. Rocas, P., Fernández, Y., Schwartz, S., Jr., Abasolo, I., Rocas, J., and Albericio, F. (2015). Multifunctionalized polyurethane-polyurea nanoparticles: hydrophobically driven self-stratification at the o/w interface modulates encapsulation stability. J. Mater. Chem. B *3*, 7604–7613.

14. Rocas, P., Hoyos-Nogués, M., Rocas, J., Manero, J.M., Gil, J., Albericio, F., and Mas-Moruno, C. (2015). Installing multifunctionality on titanium with RGD-decorated polyurethane-polyurea Roxithromycin loaded nanoparticles: toward new Osseointegrative therapies. Adv. Healthc. Mater. *4*, 1956–1960.

15. Öörni, K., Rajamäki, K., Nguyen, S.D., Lähdesmäki, K., Plihtari, R., Lee-Rueckert, M., and Kovanen, P.T. (2015). Acidification of the intimal fluid: the perfect storm for atherogenesis. J. Lipid Res. *56*, 203–214.

16. Mollazadeh, S., Mackiewicz, M., and Yazdimamaghani, M. (2021). Recent advances in the redox-responsive drug delivery nanoplatforms: a chemical structure and physical property perspective. Mater. Sci. Eng. C Mater. Biol. Appl. *118*, 111536.

17. Bajic, V.P., Van Neste, C., Obradovic, M., Zafirovic, S., Radak, D., Bajic, V.B., Essack, M., and Isenovic, E.R. (2019). Glutathione "Redox Homeostasis" and its Relation to Cardiovascular Disease. Oxid. Med. Cell. Longev. *2019*.

18. Donnini, D., Perrella, G., Stel, G., Ambesi-Impiombato, F.S., and Curcio, F. (2000). A new model of human aortic endothelial cells *in vitro*. Biochimie *82*, 1107–1114.

19. Augustine, R., Hasan, A., Primavera, R., Wilson, R.J., Thakor, A.S., and Kevadiya, B.D. (2020). Cellular uptake and retention of nanoparticles: insights on particle properties and interaction with cellular components. Mater. Today Commun. *25*, 101692.

20. Davies, P.F. (2009). Hemodynamic shear stress and the endothelium in cardiovascular pathophysiology. Nat. Clin. Pract. Cardiovasc. Med. *6*, 16–26.

21. Howard, M., Zern, B.J., Anselmo, A.C., Shuvaev, V.V., Mitragotri, S., and Muzykantov, V. (2014). Vascular targeting of nanocarriers: perplexing aspects of the seemingly straightforward paradigm. ACS Nano *8*, 4100–4132.

22. Haute, D.V., and Berlin, J.M. (2017). Challenges in realizing selectivity for nanoparticle biodistribution and clearance: lessons from gold nanoparticles. Ther. Deliv. *8*, 763–774.

23. Forman, H.J., Zhang, H., and Rinna, A. (2009). Glutathione: overview of its protective roles, measurement, and biosynthesis. Mol. Aspects Med. *30*, 1–12.

24. Maillard, J., Klehs, K., Rumble, C., Vauthey, E., Heilemann, M., and Fürstenberg, A. (2021). Universal quenching of common fluorescent probes by water and alcohols. Chem. Sci. *12*, 1352–1362.

25. Lapenna, D., de Gioia, S., Ciofani, G., Mezzetti, A., Ucchino, S., Calafiore, A.M., Napolitano, A.M., Di Ilio, C., and Cuccurullo, F. (1998). Glutathione-related antioxidant defenses in human atherosclerotic plaques. Circulation *97*, 1930–1934.

26. Flórez-Grau, G., Rocas, P., Cabezón, R., España, C., Panés, J., Rocas, J., Albericio, F., and Benítez-Ribas, D. (2016). Nanoencapsulated budesonide in self-stratified polyurethane-polyurea nanoparticles is highly effective in inducing human tolerogenic dendritic cells. Int. J. Pharm. *511*, 785–793.

27. Rocas, P., Fernández, Y., García-Aranda, N., Foradada, L., Calvo, P., Avilés, P., Guillén, M.J., Schwartz, S., Jr., Rocas, J., Albericio, F., and Abasolo, I. (2018). Improved pharmacokinetic profile of lipophilic anti-cancer drugs using αvβ3-targeted polyurethane-polyurea nanoparticles. Nanomedicine. *14*, 257–267.

28. Verma, A., and Stellacci, F. (2010). Effect of surface properties on nanoparticle–cell interactions. Small *6*, 12–21.

29. Saha, K., Kim, S.T., Yan, B., Miranda, O.R., Alfonso, F.S., Shlosman, D., and Rotello, V.M. (2013). Surface functionality of nanoparticles determines cellular uptake mechanisms in mammalian cells. Small *9*, 300–305.

30. Han, J., Weisbrod, R.M., Shao, D., Watanabe, Y., Yin, X., Bachschmid, M.M., Seta, F., Janssen-Heininger, Y.M.W., Matsui, R., Zang, M., et al. (2016). The redox mechanism for vascular barrier dysfunction associated with metabolic disorders: glutathionylation of Rac1 in endothelial cells. Redox Biol. *9*, 306–319.

STAR★METHODS

KEY RESOURCES TABLE

REAGENT or RESOURCE	SOURCE	IDENTIFIER
Chemicals, peptides, and recombinant proteins		
2,2′-dihydroxyethyl disulfide (DEDS)	Sigma Aldrich (St Louis, USA)	Cat# 380474
YMER N120	Perstorp (Malmö, Sweden)	CAS: 131483-27-7
Jeffcat DPA	Sigma Aldrich (St Louis, USA)	Cat# 24866577
Isophorone diisocyanate	Quimidroga (Barcelona, Spain)	CAS: 4098-71-9
Dry tetrahydrofuran (THF)	Sigma Aldrich (St Louis, USA)	Cat# 401757
Genamin TAP 100D	Clariant (Barcelona, Spain)	Cat#SXR024495
1,1′-dioctadecyl-3,3,3′,3′-tetramethylindocarbocyanine perchlorate	Thermo Fisher Scientific (Waltham, MA)	Cat#H55957.MC
Tributyrin	TCI Chemical (Tokyo, Japan)	Cat# T0364
L-Lysine	Sigma Aldrich (St Louis, USA)	Cat# L5626
Diethylenetriamine (DETA)	Sigma Aldrich (St Louis, USA)	Cat# 93856
EGM™-2 Endothelial Cell Growth Medium-2 BulletKit	Lonza (Walkersville, MD)	Cat# CC-3162
Hank's Balanced Salt Solution (HBSS)	Millipore Sigma (Burlington, MA)	H6648
Fluoresbrite® Multifluorescent Microspheres 0.20μm	Polysciences (Warrington, PA)	Cat# 24050-5
Formalin, buffered, 10%	Thermo Fisher Scientific (Waltham, MA)	SF100-4
Dithiothreitol (DTT)	Millipore Sigma (Burlington, MA)	DTT-RO
Diamide	Millipore Sigma (Burlington, MA)	D3648
RD Western diet	Research Diets Inc. (New Brunswick, NJ)	Cat# D12079B
Heparin	Thermo Fisher Scientific (Waltham, MA)	J16920.EXT
Paraformaldehyde	Thermo Fisher Scientific (Waltham, MA)	043368.9M
Experimental models: Cell lines		
Human aortic endothelial cells	Lonza (Walkersville, MD)	Cat# CC-2535
Experimental models: Organisms/Strains		
B6.129P2-*Apoe*^{tm1Unc}/J mice	Jackson Laboratory (Bar Harbor, ME)	Cat# 002052
Software and algorithms		
Fiji	NIH ImageJ	
Prism 9.0	GraphPad	
Other		
Leica SP5 Confocal Microscope	Boston University Cellular Imaging Core	
Panoramic MIDI II	3D Histech (Budapest, Hungary)	
Nikon wide-field epifluorescence microscope	Boston University Cellular Imaging Core	

RESOURCE AVAILABILITY

Lead contact

Further information and requests for resources and reagents should be directed to and will be fulfilled by the lead contact, Jingyan Han (jingyanh@bu.edu).

Materials availability

Further information on materials used is available from the lead contact upon request.

Data and code availability

Microscopy data reported in this paper will be shared by the lead contact upon request.

This paper does not report original code.

Any additional information required to reanalyze the data reported in this paper is available from the lead contact.

EXPERIMENTAL MODEL AND SUBJECT DETAILS

Mouse model of atherosclerosis

All experimental animal procedures were approved by the Institutional Animal Care and Use Committee of the Boston University Medical Campus. *ApoE*-deficient (*ApoE*$^{-/-}$) mice on a C57BL/6J background were purchased from the Jackson Laboratory (#002052, Bar Harbor, ME) and used as a mouse model of atherosclerosis. Only male *ApoE*$^{-/-}$ mice were used for these experiments.

Cell culture

Human aortic endothelial cells (HAECs) at passage 1 were purchased from Lonza (Walkersville, MD, Cat.# CC-2535) and cultured in an endothelial cell growth medium (EBM^{TM}-2) containing EGM^{TM}-2 SingleQuots^{TM} supplements (Lonza, Cat.# CC-3162).[30] Cells at passage 5 were used for all experiments. HAECs were starved overnight in EBM containing 0.5% fetal bovine serum before the experiments.

METHOD DETAILS

Synthesis of amphiphilic cationic polymer (P1)

2,2′-dihydroxyethyl disulfide (DEDS) (901.0 mg, 5.84 mmol, 11.68 meq), YMER N120 (12.04 g, 11.59 mmol, 23.18 meq) and N-(3-dimethylaminopropyl)-N,N′-diisopropanolamine (Jeffcat DPA) (981.3 mg, 4.50 mmol, 8.99 meq) were mixed into a round-bottomed flask with mechanical stirring at room temperature and then purged with N_2. Once homogenized, isophorone diisocyanate (IPDI) (8.14 g, 36.63 mmol, 73.24 meq) was added to the reaction flask under gentle mechanical stirring. A polyurethane formation reaction took place under these conditions until the NCO stretching band intensity did not change, monitored using IR spectroscopy. At this point, dry tetrahydrofuran (THF, 21 mL) was added to the reaction to fluidify the polymer. 1,3-diamino-N-octadecylpropane (Genamin TAP 100D) (5.99 g, 17.73 mmol, 35.45 meq) was dissolved using dry THF (5.23 mL) and added dropwise under half-moon 100 rpm mechanical stirring into another 100 mL three-necked round-bottomed flask that had previously been purged with N_2. The reaction was monitored using IR spectroscopy until the NCO stretching band intensity had completely disappeared.

Synthesis of Puua-NC-DiI

NC-DiI particles in small (SS), medium (MS), and large sizes (“big” sizes) (BS) were synthesized using a protocol developed by ECOPOL TECH, with some modifications.[6,13,14] IPDI was added to a three-necked round-bottomed flask equipped with mechanical stirring, precooled at 4°C, purged with N_2, and protected from light. 1,1′-dioctadecyl-3,3,3′,3′-tetramethylindocarbocyanine perchlorate (DiI, 3 mg, 3.21 μM), Tributyrin, polymer P1, and dry THF (in different ratios depending on the desired characteristics) were mixed in a vial and added to the round-bottomed flask, which then underwent homogenization for 10 min at 150 rpm, protected from light. An aqueous alkaline solution of L-lysine was prepared by dissolving L-lysine in Milli-Q water and adjusting the pH to 11.0 using 3 M and 1 M NaOH solutions. This solution of pH 11.0 was added to the round-bottomed flask under mechanical stirring at 250 rpm, and the polyaddition reaction was assessed after 15 min using IR spectroscopy. The organic phase was then emulsified at 300 rpm with cold Milli-Q water, and a 2% w/w aqueous solution of diethylenetriamine (DETA) was added to the emulsion to generate crosslinked NCs. Stirring was then reduced to 100 rpm. This polyaddition reaction was monitored using IR and pH measurement. Once the NCs were formed, THF was removed from the reactor at 35°C under vacuum, and dialysis purification of the NCs was carried out. Detailed synthetic procedures are described in the Supplementary Materials. Puua-NCs are characterized in Figure 1, Tables 1 and 2.

Treatments

For the NP uptake experiments, Puua-NCs in three sizes: NC-DiI-SS (small size) (14.15 ± 0.63 nm in diameter), NC-DiI-MS (medium size) (170.20 ± 44.01 nm in diameter), and NC-DiI-BS (large size)

(239.50 ± 99.78 nm in diameter) were diluted with Hank's Balanced Salt Solution (HBSS) to the indicated concentrations. Fluoresbrite® Multifluorescent Microspheres (NPs 200 nm in diameter) were purchased from Polysciences (Warrington, PA., Cat. #24050-5) and used as control NPs. The Puua-NCs and control NPs at specific concentrations were incubated with HAECs for the indicated periods of time. Thereafter, cells were washed extensively with HBSS to remove unbound particles and were then fixed using 1% paraformaldehyde before undergoing fluorescent microscopy and analysis.

To study the effect of redox status on the disassembly of Puua-NCs within HAECs, cells were pre-treated with DTT (1 mM), diamide (50 μM), or HBSS (as a control) for 60 min to alter the redox status of cells. Prior to Puua-NC incubation, cells were carefully washed with HBSS to remove extracellular DTT or diamide and to avoid possible NC breakdown before incubation. After 30 min of incubation with Puua-NCs, the cells were washed, fixed, and subjected to imaging analysis. To examine the direct effect of DTT or diamide on the disassembly of internalized Puua-NCs, the cells were incubated with Puua-NCs for 30 min and carefully washed to remove unbound NCs. Thereafter, the cells were treated with DTT or diamide for 30 min, followed by washing, fixing, and fluorescence imaging.

Whole mount *en face* aorta preparation

Eight-week-old *ApoE*$^{-/-}$ mice were fed for eight weeks on standard chow or a Western diet (WD) (purchased from Research Diets Inc., D12079B: 21% fat, 0.21% cholesterol by weight). Mice were intravenously administered with nanoparticles or DTT through the tail vein for the indicated time periods.

To harvest the aortas, the animals were euthanized by cervical dislocation, followed by perfusion of the circulatory system with 30 mL cold phosphate-buffered saline (PBS) containing heparin (40 U/mL) to remove blood components, including unbound NCs or DTT. Perfusion was then switched to 4% paraformaldehyde in PBS for 5 more min of continuous perfusion. Under a dissecting microscope, the aortas were removed of attached fat and connective tissues and opened longitudinally to expose the endothelium. To mount *en face* aorta, the opened blood vessel was placed on a cover glass with the endothelium facing down and covered by a glass slide while taking care to avoid trapping bubbles. To flatten the *en face* aorta sample, a metal weight of about 3 kg was placed on the slide for 10 min; thereafter, the coverslip was sealed by nail polish and subjected to microscopy.

Microscopy and quantification of NCs taken up by HAECs and aorta in *ApoE*$^{-/-}$ mice

For HAEC samples, images were captured with a Nikon widefield deconvolution epifluorescence microscope equipped with ×20 and ×40 objectives and filters optimized for Texas Red and DAPI. For *en face* aorta samples, microscope slides were fluorescence scanned using a Panoramic MIDI II (3D Histech, iHisto service https://www.ihisto.io/). A Leica SP5 confocal microscope (BU imaging core) was used to perform high-resolution imaging of *en face* endothelium and aortic lesions.

NP images were quantified with FIJI (NIH ImageJ) by first setting a threshold value that reflected the fluorescence value of the nanoparticle. The binary threshold images were then quantified using the FIJI function by setting resolution at 2–200 pixel^2 and circularity at 0.10–1.00.

QUANTIFICATION AND STATISTICAL ANALYSIS

Statistical analysis was performed using Prism 9.0 (GraphPad Software). Means were compared between the two groups using the Manny–Whitney *U* test. Multiple comparisons were conducted using 1-way ANOVA followed by a Dunnett test. A value of $p < 0.05$ was considered statistically significant. Additional detail of statistical tests used and error-bars on bar plots are indicated in the figure legends.